

# CONSTRAINED MAXIMUM-SINR EQUALIZATION WITH CHANNEL ESTIMATION CAPABILITIES FOR NBI-CORRUPTED OFDM SYSTEMS

Donatella Darsena

Dipartimento per le Tecnologie  
Università di Napoli Parthenope  
via Acton 38, I-80133 Napoli, Italy  
e-mail: darsena@unina.it

Giacinto Gelli, Luigi Paura and Francesco Verde

Dip. Ing. Elettronica e delle Telecomunicazioni  
Università degli Studi di Napoli Federico II  
via Claudio 21, I-80125 Napoli, Italy  
e-mail: (gelli, paura, f.verde)@unina.it.

## ABSTRACT

Constrained optimization techniques, based on the maximum signal-to-noise-plus-interference (SINR) criterion, are considered for joint equalization and narrowband interference (NBI) suppression in orthogonal frequency-division multiplexing (OFDM) systems. Specifically, we show that a recently proposed linear receiver [3], which mitigates, in the minimum mean-output-energy sense, the NBI contribution at the receiver output, can be regarded as the solution of a constrained maximum-SINR optimization criterion and, moreover, admits an interesting three-stage decomposition. This decomposition improves the receiver robustness against errors in the estimated statistics of the received data and, most important, allows one to greatly simplify the channel estimation problem. Computer simulations are carried out to illustrate the performance improvements achievable by adopting the constrained maximum-SINR equalizer, in comparison with its unconstrained counterpart.

## 1. INTRODUCTION

In many applications, orthogonal frequency-division multiplexing (OFDM) systems are expected to operate in the presence of strong narrowband interference (NBI) [1, 2, 3]. In these scenarios, the system performance becomes severely limited by interblock interference (IBI) and interchannel interference (ICI), as well as NBI. In the presence of the NBI, the conventional zero-forcing (ZF) receiver exhibits very poor performances [3], since it merely nullifies IBI and ICI, without taking any specific measure to counteract noise and NBI effects. A simple strategy to jointly counteract IBI, ICI and NBI is the adoption of bit-loading techniques at the transmitter, whose use, however, requires knowledge of the NBI parameters (i.e., bandwidth and frequency-offset) at the transmitting side, which is a quite unrealistic assumption in wireless scenarios. When the cyclic prefix (CP) length exceeds the discrete-time channel length, several data-independent reception strategies (see, e.g., [1]), which exploit the unconsumed portion of the CP not contaminated by the channel, have been proposed to increase the robustness of the receiver against NBI and noise. On the other hand, certainly more effective, but also more complex to implement, are data-dependent techniques, which are built from the received data in order to minimize noise and/or interference effects. A minimum mean-square error (MMSE) data-dependent approach to NBI rejection is proposed in [2], based on a linear interference canceler that estimates, according to the MMSE

This work was supported by the Centro Regionale di Competenza sulle Tecnologie dell'Informazione e della Comunicazione (CRdCICT).

criterion, the NBI at the receiver, under the assumption of knowing its second order statistics. A different data-dependent technique has been recently proposed in [3], where joint equalization and NBI rejection is performed by resorting to the minimum mean-output-energy (MMOE) criterion, *without* knowledge of the NBI parameters. However, the MMOE-based receiver of [3], as well as the equalizers of [1, 2], *require* a preventive estimation of the channel which, in the presence of a severe NBI, is a quite challenging task.

In this paper, after showing that the MMOE-based receiver proposed in [3] can be regarded as the result of a constrained maximum signal-to-noise-plus-interference (SINR) design, which confers robustness to the receiver when it is implemented by using short data records, we enlighten that the equalizer of [3] consists of three stages: the first stage deterministically suppresses IBI, by discarding the unconsumed portion of the CP; the second stage instead performs a data-dependent pre-filtering of the signal at the output of the first stage, in order to mitigate NBI, *without* requiring channel knowledge; the last stage, operating in a nearly NBI-free environment, recovers the desired symbols by resorting to one-tap frequency equalization (FEQ). Moreover, relying on this decomposition, we propose a simple and effective trained-based channel estimation method.

## 2. SYSTEM MODEL

Let us consider an OFDM system with  $M$  subcarriers,  $Q$  of which are utilized, whereas the remaining  $M_{vc} \triangleq M - Q$  are virtual carriers (VCs). The information data stream  $s(n)$ , with  $n \in \mathbb{Z}$ , is first converted into  $Q$  parallel substreams  $s_q(n) \triangleq s(nQ + q)$ , where the index  $q \in \{0, 1, \dots, Q - 1\}$  refers to the subcarrier. By assuming for now that the  $M_{vc}$  virtual carriers are inserted at the end of the  $n$ th data block  $\mathbf{s}(n) \triangleq [s_0(n), s_1(n), \dots, s_{Q-1}(n)]^T \in \mathbb{C}^Q$ , one obtains, after VCs insertion, the new data block  $\tilde{\mathbf{s}}(n) = \mathbf{S} \mathbf{s}(n)$ , where  $\mathbf{S} \triangleq [\mathbf{I}_Q, \mathbf{O}_{Q \times M_{vc}}]^T \in \mathbb{R}^{M \times Q}$  is tall and full-column rank, with  $\mathbf{I}_Q \in \mathbb{R}^{Q \times Q}$  denoting the identity matrix. To allow for VCs insertion in arbitrary positions, we introduce a row-permutation matrix  $\mathbf{P} \in \mathbb{R}^{M \times M}$ , i.e.,  $\tilde{\mathbf{s}}(n) = \mathbf{\Theta} \mathbf{s}(n)$ , with  $\mathbf{\Theta} \triangleq \mathbf{P} \mathbf{S} \in \mathbb{R}^{M \times Q}$ . Then, the block  $\tilde{\mathbf{s}}(n)$  is subject to the Inverse Discrete Fourier Transform (IDFT), and the resulting vector can be written as  $\tilde{\mathbf{u}}(n) = \mathbf{W}_{\text{IDFT}} \tilde{\mathbf{s}}(n) = \mathbf{W}_{\text{IDFT}} \mathbf{\Theta} \mathbf{s}(n)$ , where  $\mathbf{W}_{\text{IDFT}}$  represents the unitary symmetric IDFT matrix, and its inverse  $\mathbf{W}_{\text{DFT}} \triangleq \mathbf{W}_{\text{IDFT}}^{-1} = \mathbf{W}_{\text{IDFT}}^*$  defines the DFT matrix. Then, a cyclic prefix (CP) of length  $L_{\text{cp}}$  is inserted at the beginning of  $\tilde{\mathbf{u}}(n)$ , thus obtaining the extended block

$$\mathbf{u}(n) = \underbrace{\begin{bmatrix} \mathbf{I}_{\text{cp}} \\ \mathbf{I}_M \end{bmatrix}}_{\mathbf{T}_{\text{cp}} \in \mathbb{R}^{P \times M}} \tilde{\mathbf{u}}(n) = \underbrace{\mathbf{T}_{\text{cp}} \mathbf{W}_{\text{IDFT}} \mathbf{\Theta}}_{\mathbf{T}_0 \in \mathbb{C}^{P \times Q}} \mathbf{s}(n) = \mathbf{T}_0 \mathbf{s}(n), \quad (1)$$

where  $P \triangleq M + L_{cp}$ , matrix  $\mathbf{I}_{cp} \in \mathbb{R}^{L_{cp} \times M}$  is obtained from the identity matrix  $\mathbf{I}_M$  by picking its last  $L_{cp}$  rows, and  $\mathbf{T}_0$  is the overall full-column rank precoding matrix. Vector  $\mathbf{u}(n)$  undergoes parallel-to-serial conversion, and the resulting sequence feeds a digital-to-analog converter (DAC), operating at rate  $1/T_c = P/T$ , where  $T_c$  and  $T$  denote the sampling and the symbol period, respectively. After up-conversion, the continuous-time signal at the DAC output is transmitted over a multipath channel, which is modeled as a linear time-invariant system. If the impulse response  $h_c(\tau)$  of the composite channel spans  $L_h < P$  sampling periods, that is,  $h_c(\tau) \equiv 0$  for  $\tau \notin [0, L_h T_c]$ , after ideal carrier-frequency recovery and sampling at the rate  $1/T_c$ , the expression of the  $n$ th ( $n \in \mathbb{Z}$ ) received data block  $\tilde{\mathbf{r}}(n) \in \mathbb{C}^P$  can be expressed as (see, e.g., [3])  $\tilde{\mathbf{r}}(n) = \tilde{\mathbf{H}}_0 \mathbf{T}_0 \mathbf{s}(n) + \tilde{\mathbf{H}}_1 \mathbf{T}_0 \mathbf{s}(n-1) + \tilde{\mathbf{j}}(n) + \tilde{\mathbf{w}}(n)$ , where  $\tilde{\mathbf{j}}(n) \in \mathbb{C}^P$  and  $\tilde{\mathbf{w}}(n) \in \mathbb{C}^P$  account for the interference and thermal noise, respectively, whereas  $\tilde{\mathbf{H}}_0$  and  $\tilde{\mathbf{H}}_1 \in \mathbb{C}^{P \times P}$  are Toeplitz lower- and upper-triangular matrices (see [3] for details), depending on the discrete-time channel  $h(m) \triangleq h_c(mT_c)$ , which is a causal finite impulse response (FIR) filter of order  $L_h$ , i.e.,  $h(m) \equiv 0$  for  $m \notin \{0, 1, \dots, L_h\}$ , with  $h(0), h(L_h) \neq 0$ .

In the sequel, the following assumptions about symbols, interference, and noise are considered: **(a1)** the information symbols  $s(n)$  are modeled as a sequence of zero-mean independent and identically distributed (i.i.d.) circular random variables, with variance  $\sigma_s^2 \triangleq E[|s(n)|^2]$ ; **(a2)** the interference vector  $\tilde{\mathbf{j}}(n)$  is modeled as a zero-mean complex circular wide-sense stationary (WSS) random vector, statistically independent of  $s(n)$ ; **(a3)** the noise vector  $\tilde{\mathbf{w}}(n)$  is modeled as a zero-mean complex circular white Gaussian random vector, statistically independent of both  $s(n)$  and  $\tilde{\mathbf{j}}(n)$ , with autocorrelation matrix  $\tilde{\mathbf{R}}_{\mathbf{w}\mathbf{w}} \triangleq E[\tilde{\mathbf{w}}(n) \tilde{\mathbf{w}}^H(n)] = \sigma_w^2 \mathbf{I}_P$ .

### 3. CONSTRAINED MAXIMUM-SINR EQUALIZATION

A linear (zeroth-order) equalizer consists of a bank of  $Q$  FIR filters  $y_q(n) = \tilde{\mathbf{g}}_q^H \tilde{\mathbf{r}}(n)$ ,  $q \in \{0, 1, \dots, Q-1\}$ , where  $\tilde{\mathbf{g}}_q \in \mathbb{C}^P$  is the  $q$ th equalizer weight vector, aimed at recovering the  $q$ th symbol  $s_q(n)$  belonging to the  $n$ th symbol block  $\mathbf{s}(n)$ . The equalizer output can be expressed as  $\mathbf{y}(n) = \tilde{\mathbf{G}} \tilde{\mathbf{H}}_0 \mathbf{T}_0 \mathbf{s}(n) + \tilde{\mathbf{G}} \tilde{\mathbf{H}}_1 \mathbf{T}_0 \mathbf{s}(n-1) + \tilde{\mathbf{G}} [\tilde{\mathbf{j}}(n) + \tilde{\mathbf{w}}(n)]$ , with  $\mathbf{y}(n) \triangleq [y_0(n), y_1(n), \dots, y_{Q-1}(n)]^T \in \mathbb{C}^Q$  and  $\tilde{\mathbf{G}} \triangleq [\tilde{\mathbf{g}}_0, \tilde{\mathbf{g}}_1, \dots, \tilde{\mathbf{g}}_{Q-1}]^H \in \mathbb{C}^{Q \times P}$ . After equalization, the  $q$ th entry of  $\mathbf{y}(n)$  is quantized to the nearest (in Euclidean distance) information symbol to form the estimate of the symbol belonging to the  $q$ th data substream. Because of the FIR nature of the channel, the interblock interference (IBI) caused by the symbol block  $\mathbf{s}(n-1)$  can be deterministically suppressed by requiring that  $\tilde{\mathbf{G}} \tilde{\mathbf{H}}_1 \mathbf{T}_0 = \mathbf{O}_{Q \times Q}$  (*IBI-free condition*). Indeed, it can be shown that, by accounting for the full-column rank nature of  $\mathbf{T}_0$ , for the upper-triangular structure of  $\tilde{\mathbf{H}}_1$ , and for the fact that  $h(L_h) \neq 0$ , the IBI-free condition admits the canonical solution

$$\tilde{\mathbf{G}} = [\mathbf{O}_{Q \times L_h}, \mathbf{G}] = \mathbf{G} \underbrace{[\mathbf{O}_{N \times L_h}, \mathbf{I}_N]}_{\mathbf{R}_{L_h} \in \mathbb{R}^{N \times P}}, \quad (2)$$

where  $\mathbf{G} \triangleq [\mathbf{g}_0, \mathbf{g}_1, \dots, \mathbf{g}_{Q-1}]^H \in \mathbb{C}^{Q \times N}$  is an arbitrary matrix, with  $N \triangleq P - L_h > 0$ . Decomposition (2) leads to the *two-stage* structure for the canonical FIR IBI-free equalizer, depicted in Fig. 1, wherein the first stage evaluates  $\mathbf{r}(n) \triangleq \mathbf{R}_{L_h} \tilde{\mathbf{r}}(n) \in \mathbb{C}^N$  and hence nullifies IBI by discarding the first  $L_h$  samples of  $\tilde{\mathbf{r}}(n)$ , whereas the second stage builds  $\mathbf{y}(n) = \mathbf{G} \mathbf{r}(n)$ , where  $\mathbf{G}$  can be chosen so as to mitigate the interchannel interference (ICI), NBI and noise.

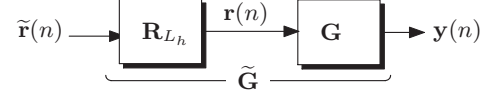


Fig. 1. The two-stage structure of the FIR IBI-free equalizer.

Accounting for the expression of  $\tilde{\mathbf{r}}(n)$ , the data block  $\mathbf{r}(n)$  at the input of the second stage is

$$\mathbf{r}(n) = \underbrace{\mathbf{H} \mathbf{T}_0}_{\mathbf{F}_0 \in \mathbb{C}^{N \times Q}} \mathbf{s}(n) + \mathbf{j}(n) + \mathbf{w}(n), \quad (3)$$

where  $\mathbf{H} \triangleq \mathbf{R}_{L_h} \tilde{\mathbf{H}}_0 \in \mathbb{C}^{N \times P}$  is the Toeplitz matrix with first column and row  $[h(L_h), 0, \dots, 0]^T$  and  $[h(L_h), \dots, h(0), 0, \dots, 0]$ , whereas  $\mathbf{j}(n) \triangleq \mathbf{R}_{L_h} \tilde{\mathbf{j}}(n) \in \mathbb{C}^N$  and  $\mathbf{w}(n) \triangleq \mathbf{R}_{L_h} \tilde{\mathbf{w}}(n) \in \mathbb{C}^N$  represent the NBI and the noise vectors.

#### 3.1. Unconstrained maximum-SINR optimization

For any  $q \in \{0, 1, \dots, Q-1\}$ , denoting with  $\bar{\mathbf{s}}_q(n) \in \mathbb{C}^{Q-1}$  the vector including all elements in  $\mathbf{s}(n)$  except for the  $(q+1)$ th entry  $s_q(n)$ , and with  $\bar{\mathbf{F}}_{0,q} \in \mathbb{C}^{N \times (Q-1)}$  the matrix including all the columns in  $\mathbf{F}_0$  except for the  $(q+1)$ th column  $\mathbf{f}_{0,q} \in \mathbb{C}^N$  and, moreover, accounting for (3), the equalizer output  $y_q(n)$  corresponding to the  $q$ th (used) subcarrier can be expressed as

$$y_q(n) = \mathbf{g}_q^H \mathbf{f}_{0,q} s_q(n) + \mathbf{g}_q^H \underbrace{[\bar{\mathbf{F}}_{0,q} \bar{\mathbf{s}}_q(n) + \mathbf{j}(n) + \mathbf{w}(n)]}_{\mathbf{d}(n) \in \mathbb{C}^N}, \quad (4)$$

where the vector<sup>1</sup>  $\mathbf{d}(n)$  collects the *overall* disturbance at the  $q$ th subcarrier, i.e., ICI, NBI and noise. A reasonable optimization criterion for deriving the  $q$ th column  $\mathbf{g}_q$  of  $\mathbf{G}$  consists of maximizing the output SINR at the  $q$ th subcarrier which, accounting for assumptions (a1)–(a3), can be written as

$$\text{SINR}_q(\mathbf{g}_q) \triangleq \frac{E[|\mathbf{g}_q^H \mathbf{f}_{0,q} s_q(n)|^2]}{E[|\mathbf{g}_q^H \mathbf{d}(n)|^2]} = \frac{\sigma_s^2 |\mathbf{g}_q^H \mathbf{f}_{0,q}|^2}{\mathbf{g}_q^H \mathbf{R}_{\mathbf{d}\mathbf{d}} \mathbf{g}_q}, \quad (5)$$

where  $\mathbf{R}_{\mathbf{d}\mathbf{d}} \triangleq E[\mathbf{d}(n) \mathbf{d}^H(n)] \in \mathbb{C}^{N \times N}$  is the autocorrelation matrix of  $\mathbf{d}(n)$ . By resorting to Cauchy-Schwarz's inequality, it can be readily proved that the optimal vector maximizing the object function (5) is given by  $\mathbf{g}_{q,\text{opt}} = \varrho_q \mathbf{R}_{\mathbf{d}\mathbf{d}}^{-1} \mathbf{f}_{0,q}$ , with  $\varrho_q \in \mathbb{C} - \{0\}$ , and the achievable (maximum) SINR at the  $q$ th subcarrier turns out to be  $\text{SINR}_{q,\text{opt}} \triangleq \text{SINR}_q(\mathbf{g}_{q,\text{opt}}) = \sigma_s^2 \mathbf{f}_{0,q}^H \mathbf{R}_{\mathbf{d}\mathbf{d}}^{-1} \mathbf{f}_{0,q}$ .

An equalizer belonging to the maximum-SINR family is [4] the MMOE solution  $\mathbf{g}_{q,\text{mmoe}} = (\mathbf{f}_{0,q}^H \mathbf{R}_{\mathbf{r}\mathbf{r}}^{-1} \mathbf{f}_{0,q})^{-1} \mathbf{R}_{\mathbf{r}\mathbf{r}}^{-1} \mathbf{f}_{0,q}$ , which minimizes the mean-output-energy  $\text{MOE}_q \triangleq E[|y_q(n)|^2]$  at the  $q$ th subcarrier, subject to  $\mathbf{g}_q^H \mathbf{f}_{0,q} = 1$ , where the imposed constraint guarantees no desired symbol cancellation. Accounting for  $\mathbf{g}_{q,\text{mmoe}}$  and let  $\odot$  denote Hadamard product of two matrices, the matrix  $\mathbf{G}$  in the second stage (see Fig. 1) assumes the form

$$\mathbf{G}_{\text{mmoe}} \triangleq [\mathbf{g}_{0,\text{mmoe}}, \mathbf{g}_{1,\text{mmoe}}, \dots, \mathbf{g}_{Q-1,\text{mmoe}}]^H = [(\mathbf{F}_0^H \mathbf{R}_{\mathbf{r}\mathbf{r}}^{-1} \mathbf{F}_0) \odot \mathbf{I}_Q]^{-1} \mathbf{F}_0^H \mathbf{R}_{\mathbf{r}\mathbf{r}}^{-1}, \quad (6)$$

<sup>1</sup>For the sake of notation simplicity, we do not explicitly indicate the dependence of  $\mathbf{d}(n)$  on the subcarrier index  $q$ .

which, by resorting to standard Lagrangian techniques, turns out to be the solution of the constrained matrix optimization criterion

$$\mathbf{G}_{\text{mmoe}} = \arg \min_{\mathbf{G} \in \mathbb{C}^{Q \times N}} E[\|\mathbf{y}(n)\|^2], \quad \text{subject to } \text{diag}(\mathbf{G} \mathbf{F}_0) = \mathbf{1}, \quad (7)$$

with  $\mathbf{1} \triangleq [1, \dots, 1] \in \mathbb{R}^Q$ . As it is well-known, another equalizer that maximizes (5) is the MMSE equalizer. In practice, the synthesis of the MMOE equalizer (or equivalently MMSE) poses two important problems. First, the matrix  $\mathbf{R}_{\text{rr}}$  is unknown and, thus, an estimate  $\hat{\mathbf{G}}_{\text{mmoe}}$  of  $\mathbf{G}_{\text{mmoe}}$  can be only obtained by replacing  $\mathbf{R}_{\text{rr}}$  in (6) with the sample autocorrelation matrix  $\hat{\mathbf{R}}_{\text{rr}}$  of  $\mathbf{r}(n)$ , estimated over  $K$  symbol intervals. Following [5], it can be shown [6] that the SINR degradation when the MMOE second stage is synthesized by using  $\hat{\mathbf{G}}_{\text{mmoe}} = [\hat{\mathbf{g}}_{0,\text{mmoe}}, \hat{\mathbf{g}}_{1,\text{mmoe}}, \dots, \hat{\mathbf{g}}_{Q-1,\text{mmoe}}]^H$  is given by

$$\text{SINR}_q(\hat{\mathbf{g}}_{q,\text{mmoe}}) = \frac{\text{SINR}_{q,\text{opt}}}{1 + \frac{N-1}{K} \text{SINR}_{q,\text{opt}}}, \quad (8)$$

which shows that, even when (ideally)  $\text{SINR}_{q,\text{opt}} \rightarrow +\infty$ , due to the effect of the finite sample-size  $K$ , the SINR saturates to the fixed value  $K/(N-1)$ . This SINR value can lead to an unacceptable bit-error rate (BER) floor already for moderate values of the number  $M$  of subcarriers. The second, and, perhaps, most important problem, is represented by the fact that the synthesis of the MMOE equalizer requires the knowledge of the composite matrix  $\mathbf{F}_0 = \mathbf{H} \mathbf{T}_0$ , which depends on the (unknown) channel matrix  $\mathbf{H}$  and on the (known) precoding matrix  $\mathbf{T}_0$ . This means that, before synthesizing the second stage in Fig. 1, one has to preliminarily estimate the channel vector  $\mathbf{h} \triangleq [h(0), h(1), \dots, h(L_h)]^T \in \mathbb{C}^{L_h+1}$  at the output of the first stage, i.e., on the basis of the vector model (3). Unfortunately, due to the NBI, conventional trained-based channel estimation techniques for OFDM systems (see, e.g., [7]) exhibit very poor performances, for low to moderate values of the signal-to-interference ratio (SIR).

### 3.2. Constrained maximum-SINR optimization

We have shown that the SINR degradation at the  $q$ th subcarrier due to the finite sample-size increases as the number of *degrees of freedom*  $N-1$  of the MMOE equalizer increases. A simple and effective way to reduce this degradation is thus to suitably reduce the degrees of freedom of the second stage, which is equivalent to adding constraints to the matrix optimization problem (7). So doing, one obtains a different second stage which is referred hereinafter to as the *constrained* MMOE (CMMOE) equalizer. On the other hand, as it is intuitively expected, reducing the number of the degrees of freedom entails a reduction of the disturbance (i.e., ICI, NBI and noise) suppression capabilities with respect to the MMOE equalizer since, in the ideal situation when  $\mathbf{R}_{\text{rr}}$  is perfectly known, the CMMOE equalizer does not maximize the output SINR for each subcarrier. A CMMOE equalizer was recently proposed in [3] for pure CP-based OFDM systems in the presence of NBI, wherein the equalizer's synthesis in the second stage is carried out by minimizing the same object function in (7), subject to the *ICI-free constraint*, namely  $\mathbf{G}_{\text{cmmoe}} = \arg \min_{\mathbf{G} \in \mathbb{C}^{Q \times N}} E[\|\mathbf{y}(n)\|^2]$ , subject to  $\mathbf{G} \mathbf{F}_0 = \mathbf{I}_Q$ , whose solution is given by  $\mathbf{G}_{\text{cmmoe}} = (\mathbf{F}_0^H \mathbf{R}_{\text{rr}}^{-1} \mathbf{F}_0)^{-1} \mathbf{F}_0^H \mathbf{R}_{\text{rr}}^{-1}$ . The CMMOE equalizer exhibits two interesting properties which were not evidenced in [3]. First of all, as it is previously stated and as it is also shown experimentally in Section 4, incorporation of the ICI-free constraint renders the estimated filtering matrix  $\hat{\mathbf{G}}_{\text{cmmoe}}$  more robust against errors in sample autocorrelation matrix  $\hat{\mathbf{R}}_{\text{rr}}$ , i.e., in comparison with the MMOE equalizer, the BER floor of the estimated CMMOE equalizer is significantly less marked. It is worth

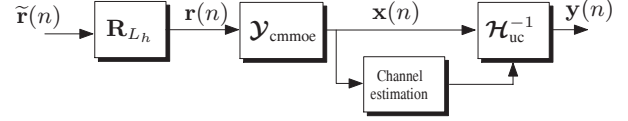


Fig. 2. The three-stage structure of the IBI-free CMMOE equalizer.

noting that, for the problem at hand, conventional correlation structured techniques for improving the estimation accuracy of  $\mathbf{R}_{\text{rr}}$  cannot be applied, due to the unknown structure of the NBI. The second property regards the channel estimation issue. Preliminarily, we observe that, when  $L_{\text{cp}} \geq L_h$ , matrix  $\mathbf{F}_0$  can be linearly parameterized as  $\mathbf{F}_0 = \mathbf{Q}_0 \mathcal{H}_{\text{uc}}$ , with  $\mathbf{Q}_0 \triangleq \Phi \mathbf{W}_{\text{IDFT}} \Theta \in \mathbb{C}^{N \times Q}$  and  $\Phi \triangleq [\mathbf{I}_\phi^T, \mathbf{I}_M]^T \in \mathbb{R}^{N \times M}$ , where  $\mathbf{I}_\phi \in \mathbb{R}^{(L_{\text{cp}} - L_h) \times M}$  is obtained from  $\mathbf{I}_M$  by picking its last  $L_{\text{cp}} - L_h$  rows and the diagonal matrix  $\mathcal{H}_{\text{uc}} \triangleq \text{diag}[H(e^{j\frac{2\pi}{M}i_0}), H(e^{j\frac{2\pi}{M}i_1}), \dots, H(e^{j\frac{2\pi}{M}i_{Q-1}})]$  collects the values of the transfer function  $H(z) \triangleq \sum_{n=0}^{L_h} h(n) z^{-n}$  at each used subcarrier. Observe that  $\mathbf{Q}_0$  is a full column rank *known* matrix, whereas matrix  $\mathcal{H}_{\text{uc}}$  is *unknown* and it is assumed to be non-singular in the sequel. Relying on this parameterization, one has [6]

$$\mathbf{G}_{\text{cmmoe}} = \mathcal{H}_{\text{uc}}^{-1} \underbrace{(\mathbf{Q}_0^H \mathbf{R}_{\text{rr}}^{-1} \mathbf{Q}_0)^{-1} \mathbf{Q}_0^H \mathbf{R}_{\text{rr}}^{-1}}_{\mathbf{Y}_{\text{cmmoe}} \in \mathbb{C}^{Q \times N}}. \quad (9)$$

Interestingly, eq. (9) leads to the *three-stage* structure for the IBI-free CMMOE equalizer, depicted in Fig. 2. The first stage is the same as that reported in Fig. 1 and is aimed at deterministically suppressing the IBI. The second stage performs a linear filtering of the vector  $\mathbf{r}(n)$  and its input-output relationship is  $\mathbf{x}(n) = \mathbf{Y}_{\text{cmmoe}} \mathbf{r}(n)$ . Remarkably, matrix  $\mathbf{Y}_{\text{cmmoe}}$  can be regarded as the solution of the constrained optimization  $\mathbf{Y}_{\text{cmmoe}} = \arg \min_{\mathbf{Y} \in \mathbb{C}^{Q \times N}} E[\|\mathbf{Y} \mathbf{r}(n)\|^2]$  subject to  $\mathbf{Y} \mathbf{Q}_0 = \mathbf{I}_Q$ . In other words, the second stage in Fig. 2 suppresses the NBI contribution, by minimizing its output power, subject to the linear matrix constraint  $\mathbf{Y} \mathbf{Q}_0 = \mathbf{I}_Q$  which is aimed at preserving the desired symbol block  $\mathbf{s}(n)$  in (3), *without* requiring channel knowledge. Therefore, if  $\mathbf{Y}_{\text{cmmoe}}$  is able to suitably suppress the NBI, the nearly NBI-free output of the second stage is given by

$$\mathbf{x}(n) \approx \mathcal{H}_{\text{uc}} \mathbf{s}(n) + \mathbf{Y}_{\text{cmmoe}} \mathbf{w}(n) = \mathbf{S}(n) \mathcal{W} \mathbf{h} + \mathbf{Y}_{\text{cmmoe}} \mathbf{w}(n), \quad (10)$$

where  $\mathbf{S}(n) \triangleq \text{diag}[s_0(n), s_1(n), \dots, s_{Q-1}(n)]$  and the  $[\mathcal{W}]_{i,\ell}$  entry of  $\mathcal{W} \in \mathbb{C}^{Q \times L_h}$  is given by  $[\mathcal{W}]_{i,\ell} = e^{-j2(\pi/N)i\ell}$ , where  $i \in \mathcal{J}_{\text{uc}}$ , with  $\mathcal{J}_{\text{uc}} \triangleq \{i_0, i_1, \dots, i_{Q-1}\}$  denoting the used subcarrier positions, and  $\ell \in \{0, 1, \dots, L_h\}$ . Thus, the last stage has simply to perform one-tap FEQ for the used subcarriers by means of the diagonal matrix  $\mathcal{H}_{\text{uc}}^{-1}$ . As it is apparent from (9), when  $M_{\text{vc}} = 0$  and  $L_{\text{cp}} = L_h$ , the CMMOE receiver boils down to the conventional ZF one. As regards the equalizer complexity, observe that, with respect to the conventional ZF equalizer, the additional computational load of the CMMOE receiver lies in the synthesis of the data-dependent component  $\mathbf{Y}_{\text{cmmoe}}^{(b)}$ . The three-stage decomposition of the CMMOE equalizer shows that, as reported in Fig. 2, channel estimation can be conveniently performed at the output of the second stage [i.e., on the basis of (10)] rather than at the output of the first stage. Therefore, let us assume that the data block  $\mathbf{s}(\bar{n})$ , with  $\bar{n} \in \{0, 1, \dots, K-1\}$ , contains  $Q$  training symbols which are known at the receiver, we propose to estimate the channel vector  $\mathbf{h}$  by means of the following least-squares (LS) optimization problem

$$\hat{\mathbf{h}} = \arg \min \|\mathbf{x}(\bar{n}) - \mathbf{S}(\bar{n}) \mathcal{W} \mathbf{h}\|^2, \quad (11)$$

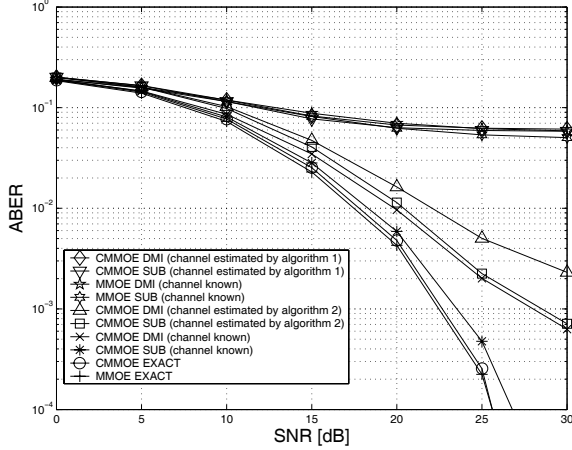


Fig. 3. ABER versus SNR.

whose solution is  $\hat{\mathbf{h}} = [\mathbf{W}^H \mathbf{S}^H(\bar{\mathbf{n}}) \mathbf{S}(\bar{\mathbf{n}}) \mathbf{W}]^{-1} \mathbf{W}^H \mathbf{S}^H(\bar{\mathbf{n}}) \mathbf{x}(\bar{\mathbf{n}})$ . In practice, the third stage performs FEQ by means of the diagonal matrix  $\hat{\mathbf{H}}_{uc}^{-1}$ , whose entries are given by the transfer function of the estimated channel  $\hat{\mathbf{h}}$ , evaluated at each used subcarrier  $\{e^{j\frac{2\pi}{M}iq}\}_{q=0}^{Q-1}$ .

#### 4. SIMULATION RESULTS

We consider a pure CP-based OFDM system employing  $M = Q = 32$  subcarriers, with a 16-QAM signaling and a CP of length  $L_{cp} = 10$ , and transmitting over a fourth-order nonminimum-phase FIR channel modeled as in [3]. The baseband continuous-time NBI is modeled as a QPSK signal, employing a raised cosine modulation pulse, with symbol period  $T_I = T/2$  and carrier frequency-offset (with respect to the OFDM system)  $f_I = 4.5/T_c$ ; in this case, the NBI exhibits a null-to-null bandwidth equal to  $B_I = 8/(PT_c)$  and, thus, corrupts about six OFDM subcarriers. Accordingly to (3), the signal-to-noise ratio is defined as  $\text{SNR} \triangleq \sigma_s^2 \|\mathbf{F}_0\|^2 / (N \sigma_w^2)$ , whereas the SIR is defined as  $\text{SIR} \triangleq \sigma_s^2 \|\mathbf{F}_0\|^2 / E[\|j(n)\|^2]$ . As a figure of merit for equalization, we adopt the average BER (ABER), defined as  $\text{ABER} \triangleq Q^{-1} \sum_{q=0}^{Q-1} \text{BER}^{(q)}$ , where  $\text{BER}^{(q)}$  is the BER relative to the  $q$ th used subcarrier, which is numerically evaluated by averaging over  $10^6$  OFDM symbols. Instead, to evaluate the channel estimation error, we adopt the (normalized) mean-squared error (MSE), defined as  $\text{MSE} \triangleq E[\|\mathbf{h} - \hat{\mathbf{h}}\|^2] / (L_h + 1)$ , with  $L_h = 4$ , which is evaluated by averaging over 200 Monte Carlo trials.

In Fig. 3, we compare the performances of the CMMOE and the MMOE equalizers, as function of the SNR, where the SIR is kept constant to 5 dB. Fig. 3 shows that, under ideal conditions (i.e., perfect knowledge of the channel impulse response and of the autocorrelation matrix  $\mathbf{R}_{rr}$ ), the CMMOE and the MMOE equalizers (referred to as “CMMOE EXACT” and “MMOE EXACT”) exhibit comparable performances, with the “MMOE EXACT” equalizer slightly outperforming the “CMMOE EXACT”. To consider a more realistic scenario, in the same figure we report the performances of the CMMOE and MMOE receivers, when the autocorrelation matrix  $\mathbf{R}_{rr}$  is estimated from  $K = 400$  OFDM symbols (referred to as “DMI”) with channel known. To reduce the effects of estimation error in  $\hat{\mathbf{R}}_{rr}$ , we consider also the subspace-based implementation [8] of the CMMOE and MMOE equalizers (referred to as “SUB”). Results of Fig. 3 show that both the “CMMOE DMI (channel known)” and “CMMOE SUB (channel known)” equalizers significantly outperform their corresponding MMOE counterparts.

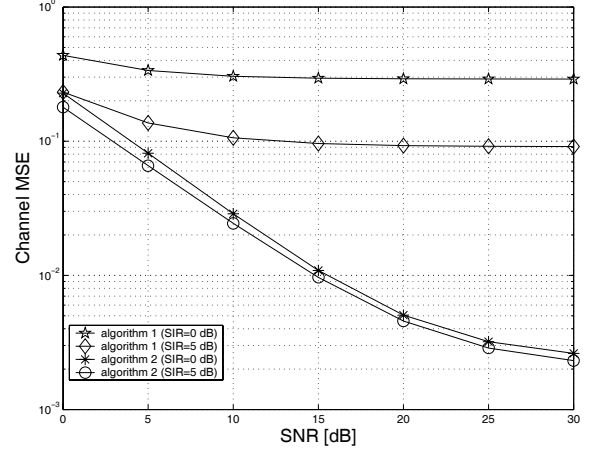


Fig. 4. Channel MSE versus SNR.

By virtue of this fact, in the same plot, we present only the performances of the “CMMOE DMI” and “CMMOE SUB” equalizers, with LS channel estimation performed at the output of the first stage as in [7] (referred to as “algorithm 1”) and, according to (11), at the output of the second stage (referred to as “algorithm 2”). Results of Fig. 3 show that the performances of both the finite-sample CMMOE equalizers are unacceptable when the channel is estimated by algorithm 1, whereas the same equalizers, with channel estimated by algorithm 2, perform satisfactorily, exhibiting only a moderate penalty with respect to their ideal counterparts “CMMOE DMI (channel known)” and “CMMOE SUB (channel known)”. Finally, in Fig. 4, we report the channel MSE as a function of the SNR, for SIR= 0 dB and SIR= 5 dB. The proposed LS channel estimation method [see (11)] significantly outperforms the approach of [7], exhibiting a slight sensibility to the SIR values.

#### 5. REFERENCES

- [1] A. J. Redfern, “Receiver window design for multicarrier communication systems,” *IEEE J. Select. Areas Commun.*, vol. 20, pp. 1029–1036, June 2002.
- [2] R. Nilsson, F. Sjöberg, and J. P. LeBlanc, “A rank-reduced LMMSE canceller for narrowband interference suppression in OFDM-based systems,” *IEEE Trans. Communications*, vol. 51, no. 12, pp. 2126–2140, Dec. 2003.
- [3] D. Darsena, G. Gelli, L. Paura, F. Verde, “NBI-resistant zero-forcing equalizers for OFDM systems”, *IEEE Commun. Letters*, vol. 53, pp. 744-746, Aug. 2005.
- [4] M. Honig, U. Madhow, and S. Verdù, “Blind adaptive multiuser detection,” *IEEE Trans. Inform. Theory*, vol. 41, pp. 944–960, July 1995.
- [5] M. Wax and Y. Anu, “Performance analysis of the minimum variance beamformer,” *IEEE Trans. Signal Processing*, pp. 928–937, April 1996.
- [6] D. Darsena, G. Gelli, L. Paura, F. Verde, “Maximum-SINR NBI-resistant receivers for wireless OFDM systems”, submitted to *IEEE Trans. Signal Processing*.
- [7] M. Morelli and U. Mengali, “A comparison of pilot-aided channel estimation methods for OFDM systems,” *IEEE Trans. Signal Processing*, vol. 49, pp. 3065–3073, Dec. 2001.
- [8] X. Wang and H. V. Poor, “Blind multiuser detection: a subspace approach,” *IEEE Trans. Inform. Theory*, vol. 44, pp. 677–690, March 1998.